



Dorsal root ganglia volume is increased in patients with the Fabry-related *GLA* variant p.D313Y

Tim Godel¹ · Philipp Bäumer^{1,2} · Katharina Stumpfe³ · Nicole Muschol³ · Moritz Kronlage¹ · Merle Brunnée¹ · Jennifer Kollmer¹ · Sabine Heiland¹ · Martin Bendszus¹ · Victor-Felix Mautner⁴

Received: 13 January 2019 / Revised: 24 February 2019 / Accepted: 26 February 2019 / Published online: 4 March 2019
© Springer-Verlag GmbH Germany, part of Springer Nature 2019

Abstract

Purpose To examine dorsal root ganglia and proximal nerve segments in patients carrying the Fabry-related *GLA*-gene variant p.D313Y in comparison to patients with classical Fabry mutations and healthy controls by morphometric and functional magnetic resonance neurography.

Methods This prospective multicenter study examines the lumbosacral dorsal root ganglia and sciatic nerve in 11 female p.D313Y patients by a standardized magnetic resonance neurography protocol at 3 T. Volumes of dorsal root ganglia L3 to S2, permeability of dorsal root ganglia L5 and S1, and spinal nerve L5 as well as cross-sectional area of the sciatic nerve were assessed and compared to 10 females carrying a classical Fabry mutation and 16 healthy female controls.

Results Compared to healthy controls, dorsal root ganglia volumes of p.D313Y females were enlarged by 53% (L3), 48% (L4), 43% (L5), 57% (S1) ($p < 0.001$), and 55% (S2) ($p < 0.05$), but less pronounced compared to females carrying a classical Fabry mutation. Compared to healthy controls, p.D313Y patients showed no changes of dorsal root ganglia vascular permeability, while patients with a classical Fabry mutation showed a distinct decrease ($p < 0.05$). Sciatic nerve cross-sectional area was mildly increased by 6% in p.D313Y as well as in classical Fabry patients ($p < 0.05$).

Conclusions Patients carrying the *GLA*-gene variant p.D313Y show distinctly enlarged dorsal root ganglia, while vascular permeability remains within normal limits. Overall, these alterations partially share characteristics commonly seen in patients with a mutation causing classical FD. This suggests that p.D313Y causes a potentially treatable condition resembling an early stage of Fabry disease.

Keywords Magnetic resonance neurography · Dorsal root ganglia · Neuropathic pain · Peripheral neuropathy · Fabry disease

Introduction

Fabry disease (FD) is a life-limiting, lysosomal multi-organ storage disorder with painful small fiber neuropathy as its earliest clinical presentation. Mutations in the *GLA* gene cause a deficiency in the enzyme alpha-galactosidase A and a subsequent accumulation of glycolipids in a wide range of cell types throughout the body. More than 600 different, disease causing mutations in the *GLA* gene have been described so far, while the pathophysiological significance of the variant p.D313Y is still under debate [1].

First, this mutation was reported to be disease causing in a male patient with a classical disease presentation [2]. Subsequent studies, however, described p.D313Y as a non-pathological polymorphism that is not necessarily associated with organ manifestations or lifetime limitations which

✉ Tim Godel
Tim.godel@med.uni-heidelberg.de

¹ Department of Neuroradiology, Neurological University Clinic, Heidelberg University Hospital, Im Neuenheimer Feld 400, 69120 Heidelberg, Germany

² Center for Radiology Dia.log, Vinzenz-von-Paul Str. 8, 84503 Altötting, Germany

³ Department of Pediatrics, University Medical Center Hamburg-Eppendorf, Martinistraße 52, 20246 Hamburg, Germany

⁴ Department of Neurology, University Medical Center Hamburg-Eppendorf, Martinistraße 52, 20246 Hamburg, Germany

are commonly seen in FD [1, 3–5]. Thus, these studies recommended no additional usage of enzyme replacement or chaperone therapy as the current therapeutic options in FD to prevent major organ complications [6].

In a recent study, however, p.D313Y patients were reported to have clinical symptoms highly reminiscent to those seen in FD [7, 8]. Moreover, previous studies described the key pathophysiological role of the dorsal root ganglion (DRG) in the development of a painful neuropathy as an early and predominant symptom of major organ involvement in patients with FD [9–11].

To assess the relevance of DRG alterations in Fabry-related *GLA*-gene variant p.D313Y in comparison to patients with classical Fabry mutations and healthy controls, the present study applied morphometric and functional Magnetic Resonance Neurography (MRN) for investigation of DRG volume, permeability, as well as sciatic nerve cross-sectional area (CSA).

Patients and methods

Clinical and demographic patient data

The study was performed in accordance with the Declaration of Helsinki, approved by the institutional ethics board (S398-2012) and written informed consent was obtained from all patients. Overall, we included 11 female patients (mean age 40.2 years and range 19–75 years) carrying the Fabry-related *GLA*-gene variant p.D313Y and no additional classical Fabry mutation as confirmed by genetic testing. Moreover, the Mainz severity score index (MSSI) [12] and lyso-Gb3 level were determined in all patients (Table 1). Patients were recruited in this prospective, multicenter study between 2/2018 and 8/2018 at the International Center for Lysosomal Disorders, University Medical Center Hamburg-Eppendorf, and MRI examinations

Table 1 Patient demographics and clinical data

Patient	Age	Age at diagnosis	<i>GLA</i> mutation	Start of ERT	Neurological symptoms	Associated clinical features	MSSI	Lyso-Gb3 level (ng/ml)
1	51	48	p.D313Y	02/15	Acroparesthesia, stroke, TIA, cerebral vasculitis	Cardiovascular: mild hypertrophy of cardiac septum, enlarged left atrium, arterial hypertension Renal: creatinine elevation GI: diarrhea/constipation General: cornea verticillata (stage 1), conjunctival tortuositatis	9	3.9
2	50	48	p.D313Y	11/15	Acroparesthesia, central artery occlusion, cerebellar vascular lesion, vertigo	Cardiovascular: cardiac arrhythmia, PFO General: retinal atrophy, conjunctival tortuositatis	6	2.6
3	45	43	p.D313Y	12/16	Acroparesthesia stroke	Cardiovascular: cardiac arrhythmia	7	0.7
4	53	50	p.D313Y	–	Acroparesthesia	General: pruritus	0	0.7
5	75	73	p.D313Y	–	Acroparesthesia (occasionally)	Cardiovascular: hypertension	4	0.7
6	20	18	p.D313Y	–	Acroparesthesia (occasionally), depression, reduced activity level, mild vertigo	GI: abdominal pain, diarrhea/constipation General: edema, tinnitus	11	1.4
7	24	23	p.D313Y	–	Acroparesthesia (occasionally), mild tinnitus, mild vertigo, fatigue	GI: abdominal pain General: edema	10	1.2
8	21	18	p.D313Y	–	None		0	0.6
9	44	44	p.D313Y	–	Mild vertigo, reduced activity level	Cardiovascular: mild valve insufficiency GI: diarrhea/constipation General: angiokeratoma, hypohydrosis	9	0.9
10	19	18	p.D313Y	–	None		0	0.9
11	40	38	p.D313Y	–	Vertigo	Sudden hearing loss (3x), tinnitus	1	0.7

ERT enzyme replacement therapy, MSSI Mainz Severity Score Index [12]

were performed at the center for MR Neurography Nord as part of the Department of Neuroradiology, Heidelberg University. Patients 1–3 received bi-weekly infusions of agalsidase-alfa (0.2 mg/kg body weight). Patients 4–11 were not on enzyme replacement therapy (ERT).

16 age-matched healthy females (mean age 38.9 years; range 22–73 years) were prospectively enrolled as a control group for quantitative measurement of DRG volume and CSA of the proximal sciatic nerve. Moreover, another 16 females are part of a previously published prospective study (mean age 51.1 years; range 21–86 years) [13] and served as controls for the assessment of quantitative DRG permeability values. Inclusion criteria for healthy controls were: ≥ 18 years, no medical history suspicious for FD, absence of neuropathic pain or other sources of pain, diabetes mellitus, alcoholism, and any malignant or infectious illness as risk factors for polyneuropathy. Exclusion criteria were any contraindications for MRI. Moreover, ten females carrying a classical Fabry mutation (mean age 45.3 years; range 28–59 years) of a previously published data set [11] served as comparison group.

Imaging protocol

Examinations were conducted on a 3 T Magnetic Resonance scanner (Magnetom SKYRA, Magnetom VERIO and Magnetom TIM TRIO, Siemens Healthineers, Erlangen, Germany). All patients and healthy controls underwent MRN including:

1. A three-dimensional (3D) T2-weighted (T2w) sampling perfection with application-optimized contrasts using different flip-angle evolution (SPACE) short-tau-inversion-recovery (STIR) sequence of the lumbosacral plexus: repetition time/echo time 3.000/208 ms, inversion time 210 ms, effective echo time 68 ms, matrix size $320 \times 320 \times 104$, field of view $305 \times 305 \text{ mm}^2$, slice thickness 1.0 mm, no gap, voxel size $1.0 \times 1.0 \times 1.0 \text{ mm}^3$, and acquisition time 8:35 min, imaging the lumbosacral spine from the second lumbar vertebra to the coccyx.
2. An axial high-resolution T2-weighted turbo-spin-echo (TSE) sequence with spectral fat saturation, covering the thigh: repetition time/echo time 8470/59 ms, matrix size 512×512 , field of view $160 \times 160 \text{ mm}^2$, slice thickness 3.5 mm, voxel size $0.3 \times 0.3 \times 3.5 \text{ mm}^3$, interslice gap 0.35 mm, 45 slices, and acquisition time 7:56 min.
3. A T1-weighted, dynamic contrast-enhanced (DCE) volumetric-interpolated breath-hold examination (VIBE) sequence (repetition time/echo time 3.3/1.11 ms, flip angle 158, 24 slices, and resolution $1.3 \times 1.3 \times 3.0 \text{ mm}^3$) covering the pelvis from the upper plate of the fifth lumbar vertebra to the second sacral vertebra. Contrast agent

(Dotarem, Guerbert, France) was administered intravenously at a concentration of 0.1 mmol/kg with a flow rate of 3.5 mL/s by automated injection. A total of 24 frames were recorded with a rate of 7.46 s per frame.

A 15-channel receive/transmit spine coil, an 8-channel receive body flex coil (Siemens), and a 15-channel receive/transmit extremity coil (Invivo, Gainesville, FL) were used.

Imaging analysis

Morphometric and functional imaging analyses were performed in analogy to the previous studies [9, 11, 13]. DRG volumes were assessed in the T2 weighted, 3D image of the lumbosacral plexus by measuring the largest diameter of the L3 to S2 DRG in coronal, sagittal, and axial reformations with Osirix (Pixmeo, Bernex, Switzerland). Volumes were calculated by the following formula: volume in $\text{mm}^3 = (\text{horizontal} \times \text{sagittal} \times \text{coronal diameter})/2$, in analogy to the mathematical equation for the volume of an ellipsoid. Sciatic nerve CSA was averaged out of ten slices at the proximal thigh level by manual segmentation of the nerve circumference. Quantitative permeability characteristics (K^{trans}) of the DRGs L5, S1, and the right spinal nerve L5 were analyzed and calculated using the commercially available software plug-in IB DCE 1.2 (Imaging Biometrics, Elm Grove, USA) to Osirix.

Statistical analysis

Statistical analyses and data visualization were performed with GraphPad Prism 7.0 (GraphPad Software, La Jolla, USA). Mean values for DRG volumes L3 to S2, vascular permeability of DRGs L5 to S1, spinal nerve L5, as well as sciatic nerve CSA were calculated and tested for statistical significance using the one-way Analysis of Variance (ANOVA) with Bonferroni correction. *P* values of < 0.05 were considered significant. All results are documented as mean values \pm Standard Error of the Mean.

Results

Quantitative analyses of DRG morphology and perfusion as well as sciatic nerve CSA were assessed for a total of 11 females carrying the Fabry-related *GLA*-gene variant p.D313Y and compared to 10 females carrying a classical Fabry mutation and 16 healthy female controls (Fig. 1).

Compared to healthy controls, DRG volumes of patients carrying p.D313Y were symmetrically increased by 53% for the DRG level L3 ($151.5 \pm 40.8 \text{ mm}^3$ vs. $98.9 \pm 41.5 \text{ mm}^3$, Bonferroni-adjusted $p < 0.001$), 48% for L4 ($192.4 \pm 49.1 \text{ mm}^3$ vs. $131.1 \pm 40.8 \text{ mm}^3$,

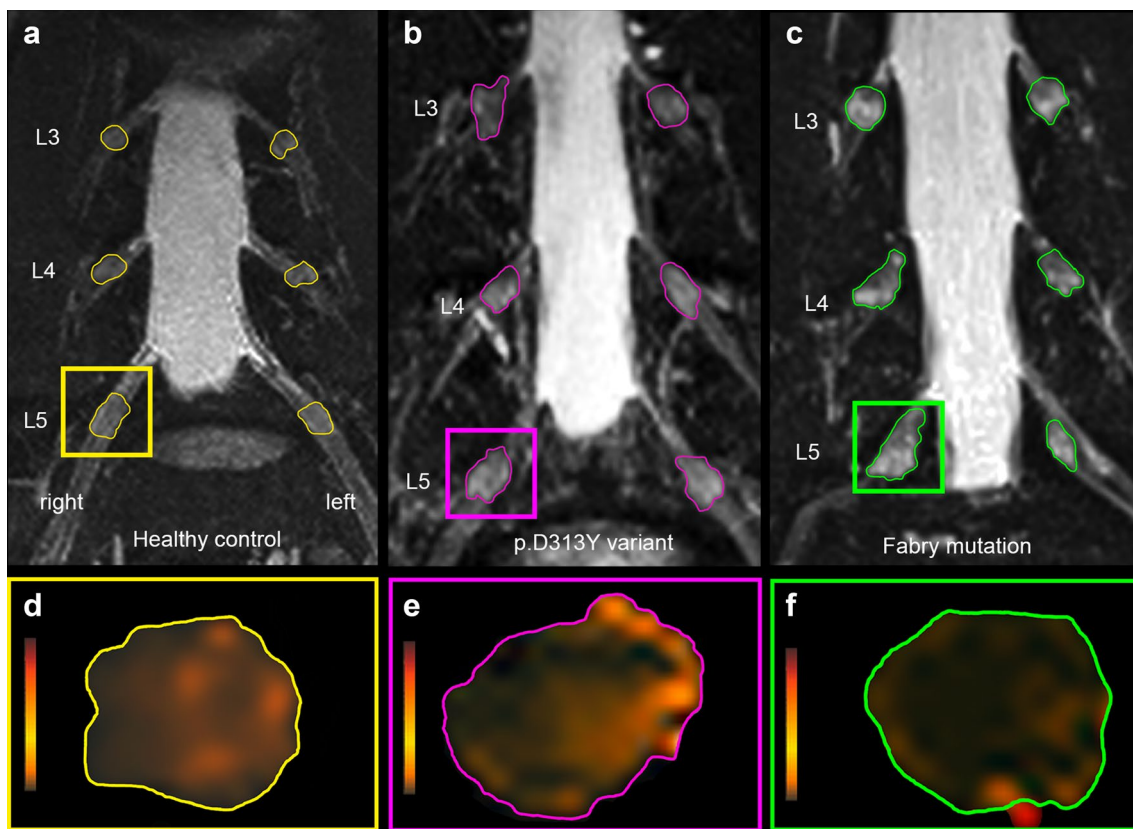


Fig. 1 Measurement of dorsal root ganglia (DRG) volume and permeability representative illustrations of DRG L3 through L5 (a–c) and permeability characteristics of the right DRG L5 (d–f). Compared to healthy controls (a, d), patients with the Fabry-related p.D313Y

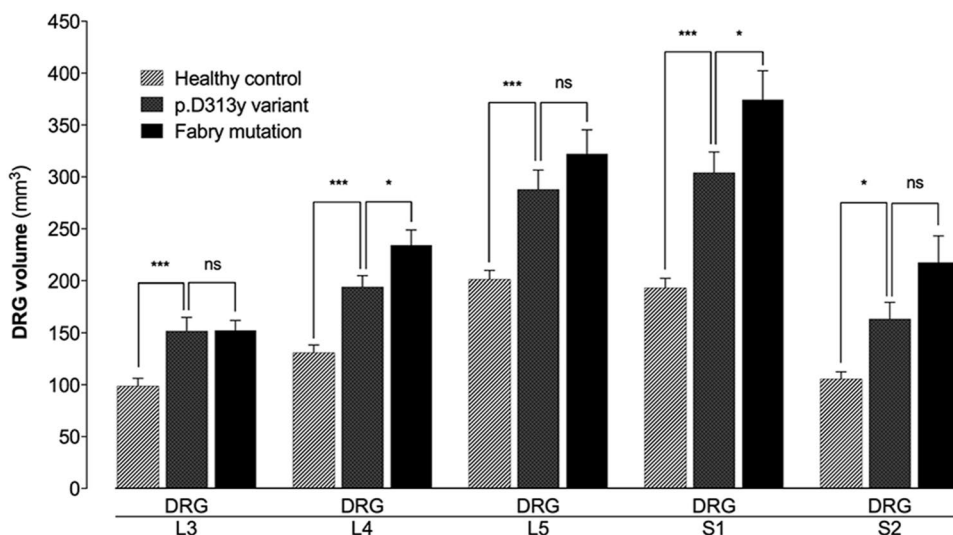
mutation show a symmetric increase in DRG volumes (b) but no changes in DRG permeability (e). Patients with a classical Fabry mutation show not only even more increased DRG volumes (c) but also a concomitant decrease in DRG permeability (f)

Bonferroni-adjusted $p < 0.001$), 43% for L5 ($288.0 \pm 87.5 \text{ mm}^3$ vs. $201.5 \pm 47.9 \text{ mm}^3$, Bonferroni-adjusted $p < 0.001$), 57% for S1 ($304.2 \pm 93.2 \text{ mm}^3$ vs. $193.4 \pm 49.7 \text{ mm}^3$, Bonferroni-adjusted $p < 0.001$), and 55% for S2 (163.5 ± 75.0

mm^3 vs. $105.8 \pm 37.9 \text{ mm}^3$, Bonferroni-adjusted $p < 0.05$) (Fig. 2).

Compared to patients with a classical Fabry mutation, DRG volumes of p.D313Y carriers were non or weak

Fig. 2 Quantitative assessment of dorsal root ganglia (DRG) volumes L3 through S2. Mean values of DRG volumes L3 through S2 were calculated level-wise for patients carrying the *GLA*-gene variant p.D313Y, patients carrying a classical Fabry mutation and healthy controls. Compared to healthy controls, p.D313Y patients showed increased DRG volumes for all levels, but less increased compared to patients carrying a classical Fabry mutation (ns non-significant, * $p < 0.05$, *** $p < 0.001$)



decreased by 0.05% for the DRG level L3 ($151.5 \pm 40.8 \text{ mm}^3$ vs. $152.3 \pm 43.2 \text{ mm}^3$, Bonferroni-adjusted $p > 0.99$), 18% for L4 ($192.4 \pm 49.1 \text{ mm}^3$ vs. $234.2 \pm 65.7 \text{ mm}^3$, Bonferroni-adjusted $p < 0.05$), 11% for L5 ($288.0 \pm 87.5 \text{ mm}^3$ vs. $322.2 \pm 103.8 \text{ mm}^3$, Bonferroni-adjusted $p = 0.48$), 19% for S1 ($304.2 \pm 93.2 \text{ mm}^3$ vs. $374.4 \pm 124.9 \text{ mm}^3$, Bonferroni-adjusted $p < 0.05$), and 25% for S2 ($163.5 \pm 75.0 \text{ mm}^3$ vs. $217.5 \pm 115.0 \text{ mm}^3$, Bonferroni-adjusted $p = 0.07$) (Fig. 2).

K^{trans} as a marker of vascular permeability of the DRG blood–neural interface showed no differences between p.D313Y patients and healthy controls for the right DRG L5 ($4.76 \pm 1.80 \cdot 10^{-3}/\text{min}$ vs. $4.72 \pm 1.21 \cdot 10^{-3}/\text{min}$, Bonferroni-adjusted $p > 0.99$), left L5 ($4.33 \pm 1.40 \cdot 10^{-3}/\text{min}$ vs. $5.15 \pm 0.96 \cdot 10^{-3}/\text{min}$, Bonferroni-adjusted $p = 0.17$), right S1 ($4.53 \pm 1.79 \cdot 10^{-3}/\text{min}$ vs. $4.79 \pm 1.12 \cdot 10^{-3}/\text{min}$, Bonferroni-adjusted $p > 0.99$), and left S1 ($4.50 \pm 1.70 \cdot 10^{-3}/\text{min}$ vs. $5.06 \pm 1.38 \cdot 10^{-3}/\text{min}$, Bonferroni-adjusted $p = 0.87$). Permeability of the spinal nerve L5 showed also no change between p.D313Y patients and healthy controls (K^{trans} SN: $2.05 \pm 0.76 \cdot 10^{-3}/\text{min}$ vs. $1.92 \pm 0.79 \cdot 10^{-3}/\text{min}$, Bonferroni-adjusted $p > 0.99$) (Fig. 3).

Compared to patients carrying the *GLA*-gen variant p.D313Y, patients with a classical Fabry mutation showed a decreased vascular permeability by 49% for the right DRG L5 ($4.76 \pm 1.80 \cdot 10^{-3}/\text{min}$ vs. $2.47 \pm 0.90 \cdot 10^{-3}/\text{min}$, Bonferroni-adjusted $p < 0.01$), by 39% for the left L5 ($4.33 \pm 1.40 \cdot 10^{-3}/\text{min}$ vs. $2.66 \pm 0.73 \cdot 10^{-3}/\text{min}$, Bonferroni-adjusted $p < 0.01$), by 43% for the right S1 ($4.53 \pm 1.79 \cdot 10^{-3}/\text{min}$ vs. $2.60 \pm 0.46 \cdot 10^{-3}/\text{min}$, Bonferroni-adjusted $p < 0.01$), and by 40% for the left S1 ($4.50 \pm 1.70 \cdot 10^{-3}/\text{min}$ vs. $2.70 \pm 0.46 \cdot 10^{-3}/\text{min}$, Bonferroni-adjusted $p < 0.05$). Spinal nerve permeability, however, showed no differences between

p.D313Y patients and patients carrying a classical Fabry mutation (K^{trans} SN: $2.05 \pm 0.76 \cdot 10^{-3}/\text{min}$ vs. $1.81 \pm 0.71 \cdot 10^{-3}/\text{min}$, Bonferroni-adjusted $p > 0.99$) (Fig. 3).

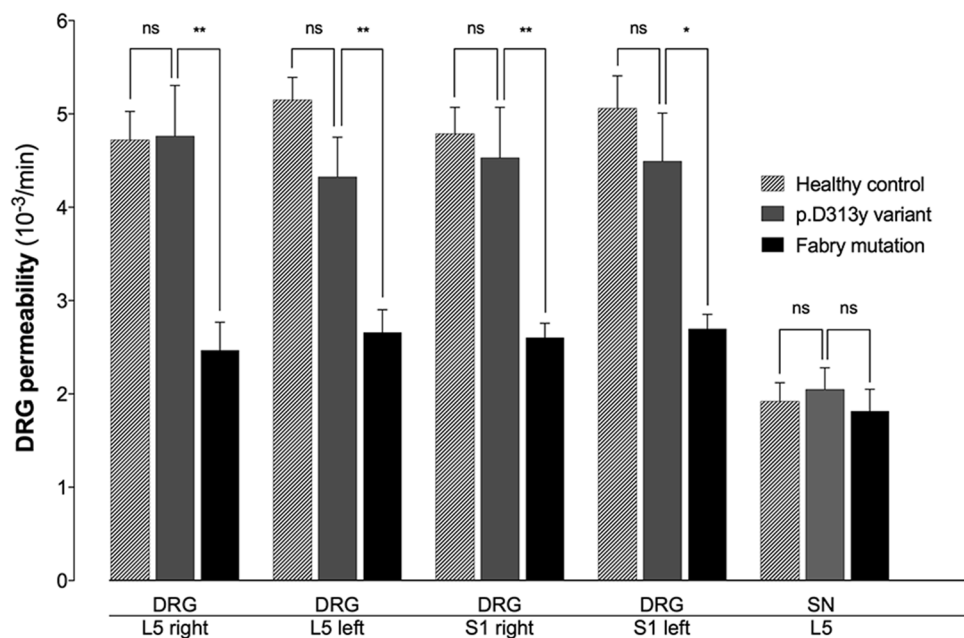
Compared to healthy controls, sciatic nerve CSA at the proximal thigh level was similarly increased by 6% in patients carrying the p.D313Y variant ($24.98 \pm 5.03 \text{ mm}^2$ vs. $23.47 \pm 4.06 \text{ mm}^2$, Bonferroni-adjusted $p < 0.05$) as well as in patients carrying a classical Fabry mutation ($24.98 \pm 4.32 \text{ mm}^2$ vs. $23.47 \pm 4.06 \text{ mm}^2$, Bonferroni-adjusted $p < 0.05$).

Discussion

By applying morphological and functional MRN, this study examined DRG volume and permeability in patients carrying the *GLA*-gene variant p.D313Y to assess the extent of measurable morphological and functional disease correlates. As a principal finding, we here report a distinct increase of DRG volumes in patients carrying p.D313Y, while vascular permeability of the DRG blood–neuronal interface remains within normal limits. Overall, these morphological and functional alterations are less pronounced compared to patients carrying a classical Fabry mutation.

The DRG is known to be a unique segment of the PNS with a high vascular supply as well as an increased endothelial permeability of the blood–neuronal interface due to large fenestrations and a relative lack of tight junction proteins [13–15]. This exception to the otherwise restricted permeability of the PNS seems to be of high clinical relevance, because endogenous and exogenous neurotoxic molecules circulating in the blood may penetrate the leaky endothelial blood–neuronal barrier and accumulate within the cell

Fig. 3 Permeability (K^{trans}) of the dorsal root ganglia (DRG) L5, S1, and spinal nerve (SN) L5. K^{trans} as a marker of the permeability of the blood–neuronal interface was assessed p.D313Y patients in comparison to patients carrying a classical Fabry mutation and healthy controls. Compared to healthy controls, no permeability changes were found in p.D313Y patients for the DRGs L5, S1, and the spinal nerve L5. Compared to p.D313Y patients, classical Fabry patients showed a decreased vascular permeability for all DRGs, but none for the spinal nerve L5 (ns non-significant, * $p < 0.05$, ** $p < 0.01$)



bodies of the primary sensory neurons. A previous histopathologic ex-vivo study in a male patient with classical FD described a distinct swelling of primary sensory neurons due to massive glycolipid accumulation within the DRG for the first time [10]. By applying high-resolution MRN, we confirmed this finding in male patients with FD in vivo [9]. Moreover, we found a concomitant decrease in vascular permeability within the DRG, most likely due to the previous massive glycolipid storage. In a subsequent study, investigating heterozygous female patients with FD, we also found severe DRG hypertrophy with a concomitant dysfunctional perfusion [11]. However, these morphological and functional alterations were less pronounced compared to Fabry males, most likely due to the X-linked inheritance resulting in partial residual enzyme activity. While the peripheral nerve segments in these patients showed only mild alterations in both genders, the cumulative effect of neurotoxic glycolipids within the DRG and a subsequent dysfunctional perfusion seem to play the key pathophysiological role in the development of neuropathy and pain in FD.

The pathophysiological significance of the Fabry-related *GLA*-gene variant p.D313Y has been controversially discussed during the last years and still remains to be solved [1]. The present study found a distinct increase in DRG volumes of p.D313Y patients. Thus, the morphological findings in this study share characteristics commonly seen in mutations causing classical FD [9, 11]. Overall, these hypertrophy rates are less pronounced compared to female patients carrying a classical Fabry mutation, most likely due to an increased residual enzyme activity as p.D313Y-mutated proteins are still transported to the lysosome and generate two-thirds of wild-type enzyme activity [1].

A cumulative effect of glycolipid storage within the DRG is in accordance with a previous study that reported p.D313Y patients to have clinical symptoms highly reminiscent to those seen in classical FD [7]. In two out of 14 patients, elevated lyso-Gb3 levels were found, a marker that has been considered to be specific for FD and suitable to identify clinically relevant mutations [16–18]. Moreover, one patient of this study group significantly improved after receiving ERT, a commonly used therapeutic option in classical FD. In addition, urinal maltose cross particles were identified in one of these patients carrying p.D313Y, a finding that is considered to be 100% specific and sensitive for FD. This patient is also part of the present study (Table 1, patient 1), showing a concomitantly elevated lyso-Gb 3 level as well as cornea verticillata as a common finding in classical FD.

A second major finding of this study is that vascular permeability within the DRG is not altered in p.D313Y patients compared to healthy controls. This finding might be a hint that glycolipid accumulation represents a pre-stage in the course of FD and occurs prior to measurable changes in

vascular permeability. This is in accordance with the pathophysiological process causing renal insufficiency in classical FD, with an accumulation of glycolipids in different renal cell types in early stages, followed by changes in permeability and glomerular filtration rate later in the course of the disease [19].

Moreover, some p.D313Y patients presented in this study showed a particular cardiovascular risk profile that is comparable to patients with classical FD [20]. A recent study reported a p.D313Y family with cerebral white matter lesions as a common finding, concluding p.D313Y as a potentially risk factor for the development of cerebral small artery disease at younger age. In this respect, a prospective study investigating patients with cerebral ischemia at younger age found an association of the p.D313Y variant and the occurrence of cryptogenic strokes [21]. Taken together, these findings raise the question whether p.D313Y patients might be at a higher risk for cardiovascular events compared to the general population. This is of particular interest as a prevalence of 0.45% for the underlying p.D313Y variant has been reported in the general population [1] and FD is commonly associated with an increased risk for the development of cardiovascular events at young age [22, 23]. Thus, new diagnostic biomarkers of disease activity, as the one presented here, have to be evaluated in the prospective longitudinal studies, not only to correlate morphological and functional DRG alterations with the occurrence of neuropathic pain as one of the earliest symptoms in FD, but also to identify patients that might be at high risk for cardiovascular events to promote the early diagnosis and therapeutic intervention.

This is of high interest, especially since causative enzyme replacement therapy (agalsidase-alpha, Replagal, Shire Human Genetic Therapies, Boston, MA; and agalsidase-beta, Fabrazyme, Genzyme Corp, Cambridge, MA) and chaperone therapy (Migalastat, Galafold, Amicus Therapeutics, Cranbury, NJ) have been introduced as safe and effective therapies in FD [24, 25]. Considering, that p.D313Y patients share partial characteristics of PNS alterations commonly seen in classical FD, the findings of this study raise the question whether patients with the Fabry-related *GLA*-gene p.D313Y variant should be monitored closely for cardiovascular complications and Fabry-specific treatment should be considered in at least those p.D313Y patients that show Fabry-related symptoms.

Conclusion

Patients with the Fabry-related *GLA*-gene variant p.D313Y show distinct enlarged DRG, while vascular permeability remains within normal limits. Overall, these alterations partially share characteristics commonly seen in patients with

mutations causing classical FD. This suggests that the *GLA*-gene variant p.D313Y causes a potentially treatable condition resembling an early stage of Fabry disease.

Acknowledgements We thank all patients for their valuable cooperation in this study. T.G. is supported by a postdoctoral fellowship from the Medical Faculty of the University of Heidelberg and received a research grant from Amicus Therapeutics. N.M. received travel grants, research grants and speaker honoraria from Shire, Sanofi Genzyme, and Amicus. J.K. received a research grant and personal fees from Alnylam Pharmaceuticals, the Olympia Morata stipend grant from the Medical Faculty of the University of Heidelberg, and lecture honoraria and financial support for conference attendance from Pfizer. She also advises for Akcea Therapeutics. M.B. received grants from the German Research Council (SFB 1158). S.H. was supported by a grant from the German Research Council (SFB 1118). V.M. was supported by a grant from the Märta and Erik Karberg Foundation for Medical Research.

Funding This research did not receive any specific grant from funding agencies in the public, commercial, or not-for-profit sectors.

Compliance with ethical standards

Conflicts of interest On behalf of all authors, the corresponding author states that there is no conflict of interest.

References

1. Yasuda M, Shabbeer J, Benson SD, Maire I, Burnett RM, Desnick RJ (2003) Fabry disease: characterization of alpha-galactosidase A double mutations and the D313Y plasma enzyme pseudodeficiency allele. *Hum Mutat* 22(6):486–492. <https://doi.org/10.1002/humu.10275>
2. Eng CM, Resnick-Silverman LA, Niehaus DJ, Astrin KH, Desnick RJ (1993) Nature and frequency of mutations in the alpha-galactosidase A gene that cause Fabry disease. *Am J Hum Genet* 53(6):1186–1197
3. Hasholt L, Ballegaard M, Bundgaard H, Christiansen M, Law I, Lund AM, Norremolle A, Krogh Rasmussen A, Ravn K, Tumer Z, Wibrand F, Feldt-Rasmussen U (2017) The D313Y variant in the *GLA* gene - no evidence of a pathogenic role in Fabry disease. *Scand J Clin Lab Invest* 77(8):617–621. <https://doi.org/10.1080/00365513.2017.1390782>
4. Oder D, Uceyler N, Liu D, Hu K, Petritsch B, Sommer C, Ertl G, Wanner C, Nordbeck P (2016) Organ manifestations and long-term outcome of Fabry disease in patients with the *GLA* haplotype D313Y. *BMJ Open* 6(4):e010422. <https://doi.org/10.1136/bmjopen-2015-010422>
5. Niemann M, Rolfs A, Giese A, Mascher H, Breunig F, Ertl G, Wanner C, Weidemann F (2013) Lyso-Gb3 indicates that the alpha-galactosidase a mutation D313Y is not clinically relevant for fabry disease. *JIMD Rep* 7:99–102. https://doi.org/10.1007/8904_2012_154
6. Eng CM, Germain DP, Banikazemi M, Warnock DG, Wanner C, Hopkin RJ, Bultas J, Lee P, Sims K, Brodie SE, Pastores GM, Strotmann JM, Wilcox WR (2006) Fabry disease: guidelines for the evaluation and management of multi-organ system involvement. *Genet Med* 8(9):539–548. <https://doi.org/10.1097/01.gim.0000237866.70357.c6>
7. Du Moulin M, Koehn AF, Golsari A, Dulz S, Atiskova Y, Paten M, Munch J, Avanesov M, Ullrich K, Muschol N (2017) The mutation p.D313Y is associated with organ manifestation in Fabry disease. *Clin Genet* 92(5):528–533. <https://doi.org/10.1111/cge.13007>
8. Selvarajah M, Nicholls K, Hewitson TD, Becker GJ (2011) Targeted urine microscopy in Anderson-Fabry disease: a cheap, sensitive and specific diagnostic technique. *Nephrol Dial Transpl* 26(10):3195–3202. <https://doi.org/10.1093/ndt/gfr084>
9. Godel T, Baumer P, Pham M, Kohn A, Muschol N, Kronlage M, Kollmer J, Heiland S, Bendszus M, Mautner VF (2017) Human dorsal root ganglion in vivo morphometry and perfusion in Fabry painful neuropathy. *Neurology* 89(12):1274–1282. <https://doi.org/10.1212/WNL.0000000000004396>
10. Gadoth N, Sandbank U (1983) Involvement of dorsal root ganglia in Fabry's disease. *J Med Genet* 20(4):309–312
11. Godel T, Kohn A, Muschol N, Kronlage M, Schwarz D, Kollmer J, Heiland S, Bendszus M, Mautner VF, Baumer P (2018) Dorsal root ganglia in vivo morphometry and perfusion in female patients with Fabry disease. *J Neurol*. <https://doi.org/10.1007/s00415-018-9053-y>
12. Whybra C, Kampmann C, Krummenauer F, Ries M, Mengel E, Miebach E, Baehner F, Kim K, Bajbouj M, Schwarting A, Gal A, Beck M (2004) The Mainz Severity Score Index: a new instrument for quantifying the Anderson-Fabry disease phenotype, and the response of patients to enzyme replacement therapy. *Clin Genet* 65(4):299–307. <https://doi.org/10.1111/j.1399-0004.2004.00219.x>
13. Godel T, Pham M, Heiland S, Bendszus M, Baumer P (2016) Human dorsal-root-ganglion perfusion measured in-vivo by MRI. *Neuroimage* 141:81–87. <https://doi.org/10.1016/j.neuroimage.2016.07.030>
14. Jimenez-Andrade JM, Herrera MB, Ghilardi JR, Vardanyan M, Melemedjian OK, Mantyh PW (2008) Vascularization of the dorsal root ganglia and peripheral nerve of the mouse: implications for chemical-induced peripheral sensory neuropathies. *Mol Pain* 4:10. <https://doi.org/10.1186/1744-8069-4-10>
15. Hirakawa H, Okajima S, Nagaoka T, Kubo T, Takamatsu T, Oyamada M (2004) Regional differences in blood-nerve barrier function and tight-junction protein expression within the rat dorsal root ganglion. *Neuroreport* 15(3):405–408
16. Aerts JM, Groener JE, Kuiper S, Donker-Koopman WE, Strijland A, Ottenhoff R, van Roomen C, Mirzaian M, Wijburg FA, Linthorst GE, Vedder AC, Rombach SM, Cox-Brinkman J, Somerharju P, Boot RG, Hollak CE, Brady RO, Poorthuis BJ (2008) Elevated globotriaosylsphingosine is a hallmark of Fabry disease. *Proc Natl Acad Sci USA* 105(8):2812–2817. <https://doi.org/10.1073/pnas.0712309105>
17. Rombach SM, Dekker N, Bouwman MG, Linthorst GE, Zwinderman AH, Wijburg FA, Kuiper S, Vd Bergh Weerman MA, Groener JE, Poorthuis BJ, Hollak CE, Aerts JM (2010) Plasma globotriaosylsphingosine: diagnostic value and relation to clinical manifestations of Fabry disease. *Biochim Biophys Acta* 1802(9):741–748. <https://doi.org/10.1016/j.bbadis.2010.05.003>
18. Niemann M, Rolfs A, Stork S, Bijnens B, Breunig F, Beer M, Ertl G, Wanner C, Weidemann F (2014) Gene mutations versus clinically relevant phenotypes: lyso-Gb3 defines Fabry disease. *Circ Cardiovasc Genet* 7(1):8–16. <https://doi.org/10.1161/CIRCGENETICS.113.000249>
19. Torra R (2008) Renal manifestations in Fabry disease and therapeutic options. *Kidney Int Suppl* 111:S29–S32. <https://doi.org/10.1038/ki.2008.522>
20. Buechner S, Moretti M, Burlina AP, Cei G, Manara R, Ricci R, Mignani R, Parini R, Di Vito R, Giordano GP, Simonelli P, Siciliano G, Borsini W (2008) Central nervous system involvement in Anderson-Fabry disease: a clinical and MRI retrospective study. *J Neurol Neurosurg Psychiatry* 79(11):1249–1254. <https://doi.org/10.1136/jnnp.2008.143693>

21. Baptista MV, Ferreira S, Pinho EMT, Carvalho M, Cruz VT, Carmona C, Silva FA, Tuna A, Rodrigues M, Ferreira C, Pinto AA, Leitao A, Gabriel JP, Calado S, Oliveira JP, Ferro JM, Investigators POYS (2010) Mutations of the GLA gene in young patients with stroke: the PORTYSTROKE study—screening genetic conditions in Portuguese young stroke patients. *Stroke* 41(3):431–436. <https://doi.org/10.1161/STROKEAHA.109.570499>
22. Kolodny E, Fellgiebel A, Hilz MJ, Sims K, Caruso P, Phan TG, Politei J, Manara R, Burlina A (2015) Cerebrovascular involvement in Fabry disease: current status of knowledge. *Stroke* 46(1):302–313. <https://doi.org/10.1161/STROKEAHA.114.006283>
23. Sims K, Politei J, Banikazemi M, Lee P (2009) Stroke in Fabry disease frequently occurs before diagnosis and in the absence of other clinical events: natural history data from the Fabry Registry. *Stroke* 40(3):788–794. <https://doi.org/10.1161/STROKEAHA.108.526293>
24. Tondel C, Bostad L, Larsen KK, Hirth A, Vikse BE, Houge G, Svarstad E (2013) Agalsidase benefits renal histology in young patients with Fabry disease. *J Am Soc Nephrol* 24(1):137–148. <https://doi.org/10.1681/ASN.2012030316>
25. Hughes DA, Nicholls K, Shankar SP, Sunder-Plassmann G, Koeiler D, Nedd K, Vockley G, Hamazaki T, Lachmann R, Ohashi T, Olivetto I, Sakai N, Deegan P, Dimmock D, Eyskens F, Germain DP, Goker-Alpan O, Hachulla E, Jovanovic A, Lourenco CM, Narita I, Thomas M, Wilcox WR, Bichet DG, Schiffmann R, Ludington E, Viereck C, Kirk J, Yu J, Johnson F, Boudes P, Benjamin ER, Lockhart DJ, Barlow C, Skuban N, Castelli JP, Barth J, Feldt-Rasmussen U (2017) Oral pharmacological chaperone migalastat compared with enzyme replacement therapy in Fabry disease: 18-month results from the randomised phase III ATTRACT study. *J Med Genet* 54(4):288–296. <https://doi.org/10.1136/jmedgenet-2016-104178>